CERN-INTC-2023-014 / INTC-P-655
11/01/2023

EUROPEAN ORGANIZATION FOR NUCLEAR RESEARCH

Proposal to the ISOLDE and Neutron Time-of-Flight Committee

Magnetic moment of ^{11}Be with ppm accuracy

January 11, 2023

A. Antušek[1], N. Azaryan[2], M. Baranowski[3], M. L. Bissell[2], M. J. Chojnacki[2], R. P. de Groote[4], A. Hurajt[5], M. Jankowski[2], G. King[6], M. Kowalska[2], S. Pastore[6], M. Pešek[2], M. Piersa-Siłkowska[2], A. Takamine[7], T. P. Treczoks[2]

[1] *Faculty of Materials Science and Technology, Slovak University of Technology, 917 24 Trnava, Slovak Republic*
[2] *Experimental Physics Department, CERN, 1211 Geneva, Switzerland*
[3] *Faculty of Physics, Adam Mickiewicz University, 61-614 Poznań, Poland*
[4] *Instituut voor Kern- en Stalingsfysica, KU Leuven, B-3001 Leuven, Belgium*
[4] *Department of Physical and Theoretical Chemistry, Faculty of Natural Sciences, Comenius University in Bratislava, 842 15 Bratislava, Slovak Republic*
[6] *Department of Physics, Washington University, St. Louis, Missouri 63130, USA*
[7] *RIKEN Nishina Center for Accelerator-Based Science, Wako, Saitama 351-0198, Japan*

Spokesperson: M. L. Bissell and M. Kowalska
Contact person: M. L. Bissell

Abstract:
Here we propose to measure the magnetic moment of the single neutron halo nucleus ^{11}Be with an accuracy of a few ppm. By combining this value with the previous high-resolution measurement of atomic hyperfine A factors, we will determine the hyperfine anomaly. In combination with state-of-the-art atomic and nuclear physics calculations, this work will provide information on the distribution of the neutron halo.

Requested shifts: [11] shifts.

1 Motivation:

The nuclear charge distribution, which provides direct information about the distribution of protons inside atomic nuclei, is routinely probed via laser spectroscopy measurements of optical isotope shifts [1]. Charge radii have already provided a wealth of information across the nuclear chart, including the evolution of closed shells, the appearance of nuclear deformation and shape coexistence.

In comparison, the nuclear magnetisation distribution can shed light on the distribution of *neutrons*. Specifically, the unpaired valence nucleons contribute and therefore the magnetisation distribution can give direct access to the orbital radius of the unpaired nucleon. This property can be determined from atomic hyperfine structure via the so-called 'hyperfine anomaly', which – in contrast to charge radii – until now has been accessible only for very few unstable nuclei.

If one could determine the distribution of magnetisation in unstable nuclei, it would be especially interesting to study it in the halo nucleus ^{11}Be, since this would provide a specific and unique way to measure the ^{11}Be neutron distribution and thus directly confirm its halo structure.

Nuclear ground state properties of ^{11}Be have been studied previously using laser spectroscopy and related techniques. The COLLAPS collaboration at ISOLDE used β-NMR in solid samples on optically-pumped Be ions to measure its magnetic moment $\mu(^{11}\text{Be}) = -1.6816(8)\mu_N$, 0.5 ‰ uncertainty), providing detailed information about the wave function of the halo neutron [2]. Here, the unexpected spin and parity as well as magnetic moment were determined, which demonstrated that the ground state configuration was predominantly of $s_{1/2}$ character. Later, the differences in charge radii between ^{7,10,11}Be and ^{9}Be were determined from optical isotope shift measurements [3]. The results obtained indicated that the charge radius of ^{11}Be is larger than that of ^{10}Be due to the motion of the proton distribution around the centre of mass of the composite core halo-neutron system. Finally, ultra-high resolution measurements of the hyperfine A factor of ^{11}Be were performed at RIKEN, with the objective of measuring the hyperfine anomaly [4].

A significant number of other experiments have also explored the ^{11}Be halo nature. These include a wide range of techniques such as decay spectroscopy and reaction studies [5–7]. However, none of the approaches applied so far were able to address directly and model independently the size of the orbit of the unpaired neutron in ^{11}Be. Here, we propose to determine this property via the the so-called magnetic hyperfine anomaly, also known as the Bohr-Weisskopf effect. This effect is a small perturbation of atomic hyperfine splitting due to the finite distribution of nuclear magnetisation [8]. In ^{11}Be, the effect is driven mainly by the unpaired halo neutron. Thus, it should be significantly larger than for stable ^{9}Be, as shown by calculations [9–11], and its magnitude should provide details about the radius of the orbital of the halo neutron. Such calculations of the hyperfine anomaly for ^{9,11}Be place the effect in the region of a few 100 ppm. We plan to combine the determined magnetic moment and hyperfine anomaly experimental results with state-of-the-art atomic (K. Pachucki [11]) and nuclear calculations (S. Pastore, G. King [12]) in order to provide firm constraints on the halo-neutron distribution.

2 Measurement principle:

The hyperfine anomaly manifests itself as a correction to the hyperfine splitting formula:

$$\Delta E = \frac{AK}{2} = A_0 * (1+\delta)(1+\epsilon)\frac{K}{2} = \mu B_0(1+\delta)(1+\epsilon)\frac{K}{2IJ},$$

where δ is the correction due to the finite distribution of charge known as the Breit–Rosenthal effect and ϵ is the magnetic hyperfine anomaly due to the finite distribution of magnetisation, which is of interest to us. In order to determine ϵ for one isotope, precise atomic calculations of the magnetic hyperfine-structure constant of a point-like nucleus, A_0, and δ are required.
The differential hyperfine anomaly, ${}^{N}\Delta^{N'}$, between two isotopes of the same element avoids the need for precise calculations of the hyperfine A_0 factor, since it can be expressed as

$$ {}^{N}\Delta^{N'} = \frac{A^N/g_I^N}{A^{N'}/g_I^{N'}} - 1 \approx \epsilon^N - \epsilon^{N'} + \delta^N - \delta^{N'}, $$

where the nuclear g-factor $g_I^N = \mu^N/(I\mu_N)$.
To determine the hyperfine anomaly, one requires an accurate measurement of the magnetic moment and that of the hyperfine structure constant (in this case both for ^{11}Be), while for the differential anomaly, the values have to be known also for a reference nucleus (here, stable ^{9}Be). The ^{9,11}Be ground state hyperfine structure constants have already been measured with sufficient precision, $A^9 = -625.008837048(10)$ MHz [13] and $A^{11} = -2677.302988(72)$ MHz [4]. The present proposal is concerned with the determination of the second ingredient required for the hyperfine anomaly, namely the magnetic moment of ^{11}Be at several parts-per-million level. To achieve this goal, we will use β-NMR in liquid samples, which – as we have recently shown – provides precise and accurate magnetic moments for short-lived nuclei [14].
The experiment will take place using the laser-polarisation and high-field β-NMR setups at the VITO beamline [15, 16], using a similar principle to our determination of the magnetic moment of ^{26}Na [14]. The ^{11}Be beam will be polarised as an ion via optical pumping between the ionic ground state and the $2p\ {}^2P_{1/2}$ level, at 313 nm [2]. The optical pumping process is demonstrated in figure 1 and as shown will be enhanced by exciting both the $F = 0$ to $F' = 1$ and $F = 1$ to $F' = 1$ hyperfine components. This will be achieved by voltage tuning different parts of the optical pumping region to bring both transitions into resonance. In the COLLAPS experiment [2] 1 % of time-averaged β-decay asymmetry was achieved via optical pumping in the same atomic transition. However, in that experiment only one F state could be excited at a time and in addition, only 1 mW of UV light was available from intra-cavity frequency doubling, which was not enough to saturate the transition. We will use an external doubling cavity (Wavetrain) which permits the generation of up to 100 mW in that frequency range (as demonstrated at 280 nm in COLLAPS Mg studies [17]). In addition, our time-resolved data acquisition system allows us to perform offline time-cuts, thus obtaining the best signal-to-noise ratio by selection of events in a given time window. Both features should allow us to observe a somewhat higher degree of asymmetry, at the several per-cent level.
The spin-polarised ion beam will then reach a thin layer of liquid, placed at 45° to vertical inside our 4.7 T superconducting magnet. The liquid used will be a low vapour-pressure ionic liquid, EMIM-DCA or BMIM-COOH. Asymmetric β emission from the polarised ^{11}Be nuclei will be recorded it two β detectors, one placed along the magnetic field and another against it. Radio-frequency excitation at the ^{11}Be Larmor frequency will destroy the spin polarisation, resulting in a decrease of β-asymmetry.
Initial optimisation of the polarisation will be performed in a Be crystal host as in reference 2. Subsequent studies will take place in a liquid sample, for which very narrow resonances will be obtained, due to the field averaging effect of molecular tumbling motion. With a 13.8 s half-life, ^{11}Be may seem long-lived for β-NMR studies, in comparison to previously investigated nuclei such as ^{11}Li [18] or ^{31}Mg [17]. However, we expect the ^{11}Be relaxation time for spin polarization to be several seconds in both solid and liquid samples, since the spin of ^{11}Be is 1/2 and thus it does not undergo relaxation due to quadrupolar interactions. We have already

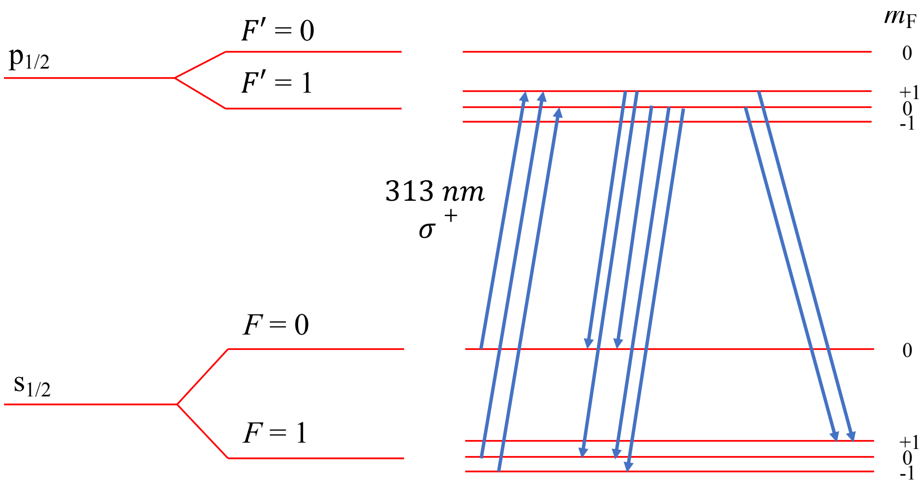

Figure 1: Optical pumping scheme for the polarisation of Be II

observed relaxation times in that range in our experimental setup in a crystal and EMIM-DCA for spin 1/2 ^{47}K, which has a 17 s half-life [16]. Depending on the relaxation time, EMIM-DCA or another ionic liquid already used at VITO, BMIM-COOH, will be used.

The ^{11}Be Larmor frequency determined in the liquid will be compared to the frequency of ^{2}H measured simultaneously, or between ^{11}Be measurements, in a small tube placed several millimetres away from the β-NMR sample. The observed difference of ^{2}H Larmor frequency and thus magnetic field, between the two positions is 1 ppm.

3 ^{11}Be magnetic moment and hyperfine anomaly derivation and interpretation

To derive the ^{11}Be magnetic moment at a ppm level from the ^{11}Be to ^{2}H frequency ratio, two paths can be taken. In the first approach, a conventional NMR measurement on stable ^{9}Be will be conducted by our collaborators at UNIGE in the same ionic liquid as that selected for ^{11}Be, which will be followed by a measurement for ^{2}H in heavy water. By using ^{9,11}Be and ^{2}H in the same hosts, respectively ionic liquid and water, all NMR shieldings cancel out and only the known difference in magnetic susceptibility of the different samples needs to be included (see reference 14 for details.) In this way, ^{2}H is used only to determine the magnetic fields at which the ^{9}Be and ^{11}Be measurements take place, while the true reference nucleus is ^{9}Be, whose magnetic moment is used to determine the ^{11}Be moment. The magnetic moment of ^{9}Be is already known with sufficient accuracy of 4 ppm, $\mu(^{9}\text{Be}) = 1.177430(5)\mu_N$. It has been derived by one of us (A. Antušek) by combining a past NMR measurement with coupled-cluster quantum-chemical calculations of beryllium NMR shielding in water.

An alternative route to derive an accurate ^{11}Be moment is by using the measured ^{11}Be/^{2}H frequency ratio together with calculated NMR shieldings for ^{2}H in heavy water and Be in the selected ionic liquid. The former is known theoretically with very high accuracy [19], while the latter will be calculated by us (A. Antušek and A. Hurajt). We expect to reach an uncertainty smaller than 3 ppm. A similar 3 ppm uncertainty in shielding was recently achieved for the sodium ion in EMIM-DCA [K. Dziubinska-Kühn *et al.*, to be submitted], using molecular

dynamics and density functional theory calculations.
In this way, both the absolute magnetic moment $\mu(^{11}\mathrm{Be})$ relevant to the hyperfine anomaly and also the ratio of g-factors $g_I(^{11}Be)/g_I(^{9}Be)$ relevant to the differential anomaly will be determined with statistical and systematic uncertainties at the few ppm level.

Quantum Monte Carlo calculation of the hyperfine anomaly: State-of-the-art Variational Monte Carlo, VMC and Greens Function Monte Carlo, GFMC calculations of magnetic moments successfully reproduce experimental data in several light nuclei [12]. In particular, the magnetic moment of ^{9}Be was obtained with a phenomenological nuclear interaction and found to be in good agreement with available data. The theoretical magnetic moment will require the development of unnatural parity states in ^{11}Be in VMC and GFMC which is being actively pursued for the Norfolk local chiral nuclear Hamiltonian [20]. Performing the calculation with several Norfolk model classes will allow for the assessment of nuclear model uncertainty on the theoretical magnetic moment. Recent VMC calculations of electroweak properties of $A = 11$ nuclei using the Norfolk model was found to be in good agreement with experimental data [21]. The method is capable of providing single- and two-nucleon (magnetization) densities that will aid in the interpretation of the halo structure of ^{11}Be.

The calculation of the hyperfine structure constant A_{th} in VMC and GFMC is being actively researched. At present, we can calculate leading order two-photon exchange corrections to the hyperfine splitting, *i.e.*, the Low moment, which comes from considering *only* the leading order terms in the nuclear Compton amplitude. Including other corrections, such as the vector polarizability, requires synergy between nuclear and atomic theorists and is being vigorously pursued. The importance of higher-order nuclear charge and current operators is also well-established, as they provide important two-body physics and quantum interference effects. Presently, these higher order operators are not included in the Low moment calculation; however, work to incorporate these corrections in the nuclear Compton tensor will be pursued in the future.

Absolute hyperfine anomaly for $\mu(^{11}\mathrm{Be})$: Here, we will interpret the measured magnetic moment by including it in accurate QED calculations of the hyperfine structure constant A_{th} [11] that will be compared with the previously measured value of A_{exp} [4]. A_{th} will be first derived assuming a point-like nucleus, as in reference [11], and will then include the nuclear structure calculations using GFMC, for which we are already preparing. The latter correction should bring A_{th} into agreement with A_{exp}, allowing the interpretation of the measurements in terms of the wavefunction and spacial distribution of the halo neutron. In addition, GFMC can be benchmarked to the value of the magnetic moment itself (which, however, does not require the ppm accuracy). A similar procedure will be performed for the stable non-halo ^{9}Be, for which both the magnetic moment and hyperfine structure constant are already known. Here, the effect of finite nuclear charge and magnetisation has been estimated to be about 600 ppm [11].

Differential hyperfine anomaly between $\mu(^{9}\mathrm{Be})$ and $\mu(^{11}\mathrm{Be})$: As mentioned before, the differential anomaly ϵ_{exp} requires only experimental values of g_I and A. To interpret ϵ_{exp} in terms of nuclear structure, its value should be compared to theoretical values based on different structures of both isotopes. Several ϵ_{th} values are already available in the literature [9, 10, 22]. Additionally, GFMC calculations required for the absolute hyperfine anomaly will be used to derive the differential anomaly.

4 Beamtime request

For the ^{11}Be beam, we request a UC$_x$ or Ta target with laser ionisation, for which we expect yields of about 5×10^{6} ions/μC. Although the yield at ISOLDE is relatively large for this isotope, the 13.8s half life limits the speed at which we can perform rf scans. Here we can only take one to two proton pulses per super-cycle (depending on the super-cyle length), to prevent activity from the previous pulse contaminating the following scan step. The number of requested shifts is based on our experience with liquid β-NMR at our beamline and is tabulated below:

Task	Shifts
Establish the highest possible laser polarisation and β asymmetry in ^{11}Be, using single-frequency laser polarisation and subsequently laser re-pumping.	3
Locate the correct rf resonance frequency using β-NMR in the solid-state host.	1
Measure asymmetry relaxation rates in the two potential liquid hosts, BMIM-COOH and EMIM-DCA.	1
Perform rf-modulation scans in order to locate the narrow resonance in the chosen liquid and define the final modulation-free scanning range.	2
Acquire at least three independent high-resolution scans in separate liquid samples.	4

Summary of requested shifts: 11 online + 1 offline for beam tuning.

References

[1] P. Campbell, I.D. Moore, and M.R. Pearson. Laser spectroscopy for nuclear structure physics. *Progress in Particle and Nuclear Physics*, 86:127–180, 2016.

[2] W. Geithner, S. Kappertz, M. Keim, P. Lievens, R. Neugart, L. Vermeeren, S. Wilbert, V. N. Fedoseyev, U. Koster, V. I. Mishin, and V. Sebastian. Measurement of the magnetic moment of the one-neutron halo nucleus ^{11}Be. *Physical Review Letters*, 83:3792–3795, 1 1999.

[3] W. Nörtershäuser, D. Tiedemann, M. Žáková, Z. Andjelkovic, K. Blaum, M. L. Bissell, R. Cazan, G. W. F. Drake, Ch. Geppert, M. Kowalska, J. Krämer, A. Krieger, R. Neugart, R. Sánchez, F. Schmidt-Kaler, Z.-C. Yan, D. T. Yordanov, and C. Zimmermann. Nuclear charge radii of ^{7,9,10}Be and the one-neutron halo nucleus ^{11}Be. *Phys. Rev. Lett.*, 102:062503, Feb 2009.

[4] A. Takamine, M. Wada, K. Okada, T. Sonoda, P. Schury, T. Nakamura, Y. Kanai, T. Kubo, I. Katayama, S. Ohtani, H. Wollnik, and H. A. Schuessler. Hyperfine structure constant of the neutron halo nucleus ^{11}Be. *Physical Review Letters*, 112:1–5, 2014.

[5] M. Fukuda, T. Ichihara, N. Inabe, T. Kubo, H. Kumagai, T. Nakagawa, Y. Yano, I. Tanihata, M. Adachi, K. Asahi, M. Kouguchi, M. Ishihara, H. Sagawa, and S. Shimoura. Neutron halo in ^{11}Be studied via reaction cross sections. *Physics Letters B*, 268(3):339–344, 1991.

[6] R. Anne, R. Bimbot, S. Dogny, H. Emling, D. Guillemaud-Mueller, P.G. Hansen, P. Hornshøj, F. Humbert, B. Jonson, M. Keim, M. Lewitowicz, P. Møller, A.C. Mueller, R. Neugart, T. Nilsson, G. Nyman, F. Pougheon, K. Riisager, M.-G. Saint-Laurent, G. Schrieder, O. Sorlin, O. Tengblad, and K.Wilhelmsen Rolander. Exclusive and restricted-inclusive reactions involving the ^{11}Be one-neutron halo. *Nuclear Physics A*, 575(1):125–154, 1994.

[7] Y. Hirayama, T. Shimoda, H. Izumi, H. Yano, M. Yagi, A. Hatakeyama, C.D.P. Levy, K.P. Jackson, and H. Miyatake. Structure of ^{11}Be studied in β-delayed neutron- and γ-decay from polarized ^{11}Li. *Nuclear Physics A*, 746:71–75, 2004. Proceedings of the Sixth International Conference on Radioactive Nuclear Beams (RNB6).

[8] Aage Bohr and V. F. Weisskopf. The influence of nuclear structure on the hyperfine structure of heavy elements. *Phys. Rev.*, 77:94–98, Jan 1950.

[9] Y. L. Parfenova and Ch Leclercq-Willain. Hyperfine anomaly in Be isotopes and the neutron spatial distribution: A three-cluster model for ^{9}Be. *Physical Review C - Nuclear Physics*, 72:1–7, 2005.

[10] Y. L. Parfenova and Ch Leclercq-Willain. Hyperfine anomaly in Be isotopes in the cluster model and the neutron spatial distribution. *Physical Review C - Nuclear Physics*, 72:024312, 2005.

[11] Mariusz Puchalski and Krzysztof Pachucki. Ground-state hyperfine splitting in the Be+ ion. *Physical Review A - Atomic, Molecular, and Optical Physics*, 89:1–7, 2014.

[12] S. Pastore, Steven C. Pieper, R. Schiavilla, and R. B. Wiringa. Quantum monte carlo calculations of electromagnetic moments and transitions in A$\leq$9 nuclei with meson-exchange currents derived from chiral effective field theory. *Physical Review C - Nuclear Physics*, 87:1–15, 2013.

[13] D. J. Wineland, J. J. Bollinger, and Wayne M. Itano. Laser-fluorescence mass spectroscopy. *Phys. Rev. Lett.*, 50:628–631, Feb 1983.

[14] R. D. Harding, S. Pallada, J. Croese, A. Antušek, M. Baranowski, M. L. Bissell, L. Cerato, K. M. Dziubinska-Kühn, W. Gins, F. P. Gustafsson, A. Javaji, R. B. Jolivet, A. Kanellakopoulos, B. Karg, M. Kempka, V. Kocman, M. Kozak, K. Kulesz, M. Madurga Flores, G. Neyens, R. Pietrzyk, J. Plavec, M. Pomorski, A. Skrzypczak, P. Wagenknecht, F. Wienholtz, J. Wolak, Z. Xu, D. Zakoucky, and M. Kowalska. Magnetic moments of short-lived nuclei with part-per-million accuracy: Toward novel applications of β-detected nmr in physics, chemistry, and biology. *Phys. Rev. X*, 10:041061, Dec 2020.

[15] J. Croese, M. Baranowski, M.L. Bissell, K.M. Dziubinska-Kühn, W. Gins, R.D. Harding, R.B. Jolivet, A. Kanellakopoulos, B. Karg, K. Kulesz, M. Madurga Flores, G. Neyens, S. Pallada, R. Pietrzyk, M. Pomorski, P. Wagenknecht, D. Zakoucky, and M. Kowalska. High-accuracy liquid-sample β-NMR setup at isolde. *Nuclear Instruments and Methods in Physics Research Section A: Accelerators, Spectrometers, Detectors and Associated Equipment*, 1020:165862, 2021.

[16] M. Jankowski et al. From magnetic moments and biochemistry to future β-nmr studies at vito. Invited talk at the ISOLDE Workshop and Users meeting 2022, https://indico.cern.ch/event/1183259/contributions/5110831/, 2022.

[17] G. Neyens, M. Kowalska, D. Yordanov, K. Blaum, P. Himpe, P. Lievens, S. Mallion, R. Neugart, N. Vermeulen, Y. Utsuno, and T. Otsuka. Measurement of the spin and magnetic moment of ^{31}Mg: Evidence for a strongly deformed intruder ground state. *Phys. Rev. Lett.*, 94:022501, Jan 2005.

[18] R. Neugart, D. L. Balabanski, K. Blaum, D. Borremans, P. Himpe, M. Kowalska, P. Lievens, S. Mallion, G. Neyens, N. Vermeulen, and D. T. Yordanov. Precision measurement of ^{11}Li moments: Influence of halo neutrons on the ^{9}Li core. *Phys. Rev. Lett.*, 101:132502, Sep 2008.

[19] Wåodzimierz Makulski, Marcin Wilczek, and Karol Jackowski. ^{17}O and ^{1}H NMR spectral parameters in isolated water molecules. *Phys. Chem. Chem. Phys.*, 20:22468–22476, 2018.

[20] M. Piarulli et al. Light-nuclei spectra from chiral dynamics. *Phys. Rev. Lett.*, 120(5):052503, 2018.

[21] J. Schmitt et al. Probing spin-isospin excitations in proton-rich nuclei via the ^{11}C(p,n)^{11}N reaction. *Phys. Rev. C*, 106(5):054323, 2022.

[22] T. Fujita, K. Ito, and Toshio Suzuki. Hyperfine anomaly of Be isotopes and anomalous large anomaly in ^{11}Be. *Phys. Rev. C*, 59:210–214, Jan 1999.

DESCRIPTION OF THE PROPOSED EXPERIMENT
Please describe here below the main parts of your experimental set-up:

Part of the experiment	Design and manufacturing
If relevant, write here the name of the fixed installation you will be using [Name fixed/present ISOLDE installation: VITO	☐ To be used without any modification ☒ To be modified
New UV laser system	☒ Standard equipment supplied by a manufacturer ☐ CERN/collaboration responsible for the design and/or manufacturing
UV Laser transport system	☐ Standard equipment supplied by a manufacturer ☒ CERN/collaboration responsible for the design and/or manufacturing

HAZARDS GENERATED BY THE EXPERIMENT
Additional hazard from flexible or transported equipment to the CERN site:

Domain	Hazards/Hazardous Activities		Description
Mechanical Safety	Pressure	☐	[pressure] [bar], [volume][l]
	Vacuum	☐	
	Machine tools	☐	
	Mechanical energy (moving parts)	☐	
	Hot/Cold surfaces	☐	
Cryogenic Safety	Cryogenic fluid	☐	[fluid] [m3]
Electrical Safety	Electrical equipment and installations	☐	[voltage] [V], [current] [A]
	High Voltage equipment	☐	[voltage] [V]
Chemical Safety	CMR (carcinogens, mutagens and toxic to reproduction)	☐	[fluid], [quantity]
	Toxic/Irritant	☐	[fluid], [quantity]
	Corrosive	☐	[fluid], [quantity]
	Oxidizing	☐	[fluid], [quantity]
	Flammable/Potentially explosive atmospheres	☐	[fluid], [quantity]
	Dangerous for the environment	☐	[fluid], [quantity]
Non-ionizing radiation Safety	Laser	☒	Wavetrain, class 4
	UV light	☒	
	Magnetic field	☐	[magnetic field] [T]
Workplace	Excessive noise	☐	
	Working outside normal working hours	☐	
	Working at height (climbing platforms, etc.)	☐	
	Outdoor activities	☐	

Fire Safety	Ignition sources	☐	
	Combustible Materials	☐	
	Hot Work (e.g. welding, grinding)	☐	
Other hazards			